ISBN: 978-3-95450-214-1 ISSN: 2673-5490 doi:10.18429/JACoW-IPAC2021-THPAB031

DUMP LINE LAYOUT AND BEAM DILUTION PATTERN OPTIMIZATION OF THE FUTURE CIRCULAR COLLIDER

B. Facskó*, D. Barna, Wigner Research Centre for Physics, Budapest, Hungary
E. Renner, A. Lechner, CERN, Geneva, Switzerland

Abstract

To avoid any damage to the beam dump target in the Future Circular Collider, the beam will be swept over its surface using oscillating "dilution" kickers in the x/y planes with a 90° phase difference, and an amplitude changing in time, creating a spiral pattern. The ideal pattern must have an increasing spiral pitch towards smaller radii to produce an even energy deposition density. We recommend the realization of the optimal pattern using two beating frequencies. This method enables a flat energy deposition density while only using simple independent damped oscillators. Two different, optimized beamline layouts are also presented.

INTRODUCTION

The 8.3 GJ energy stored in both beams of the Future Circular Collider hadron-hadron ring (FCC-hh) makes it necessary to sweep the extracted beam in a precisely defined way over the surface of the dump absorber. This pattern needs to be optimized to keep the size of the absorber and the dilution kickers' strength minimal while not exceeding the damage threshold of the target material. The trivial pattern is a spiral, realized by a combined horizontal and vertical kicker system with fixed frequency and changing amplitude. The ideal waveforms in the two planes are $R_{\text{ideal}}(t)\cdot\cos(2\pi f_0 t)$, where the envelope R_{ideal} is a concave function having a larger rate of change at small radii to compensate the smaller peripheral progression velocity of the spiral pattern. An inward spiral can be naturally realized by a lossy RLC circuit (a capacitor bank discharged into the kicker magnet). However, the envelope of this function is convex, with decreasing rate of change towards small radii, which leads to a higher energy deposition density. If the damage threshold of the dump absorber needs to be respected, the target would need to be larger as with an optimal energy distribution pattern. See [1] for a more detailed discussion.

A novel idea is to approximate the ideal waveform by using two slightly different frequencies in both planes. Their interference creates a beating waveform with a concave envelope. A further advantage of this concept is that the electric circuits can remain simple and uncoupled. They interfere only in their effect on the beam.

THE IDEAL DUMP PATTERN

The Concept

Write the x coordinate of the pattern in the following form:

$$x(t) = A_1 e^{-\frac{t}{\tau}} \sin\left(2\pi[f-\Delta f]t\right)\Theta(t) + A_2 e^{-\frac{t-\Delta t}{\tau}} \sin\left(2\pi f[t-\Delta t]\right)\Theta(t-\Delta t), \quad (1)$$

where A_1 and A_2 are amplitudes, τ is the time constant of the lossy circuit, f is the frequency of the oscillations, Δf is the frequency difference and Δt is a time offset between the two frequencies. Θ is the Heaviside function. The $y(t)$ function has the same formula with a 90° phase delay with respect to $x(t)$.

Figure 1 shows the energy profile of one bunch at the dump target, obtained by a FLUKA simulation. The energy deposition map of the entire bunch train is obtained by the convolution of a single bunch profile with the individual positions of the bunches.

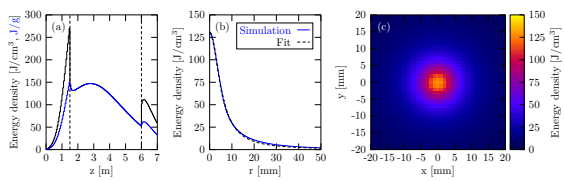

Figure 1: (a) Longitudinal profile of the maximum energy deposition density of a single bunch as a function of penetration depth. (b) Simulated and fitted radial energy deposition density profile at a depth of 375 cm. (c) Two-dimensional energy deposition density map of a single bunch.

Optimization

In order to deal with the two conflicting goals of keeping the maximum energy deposition density E_{max} of the pattern below a threshold, and the dump pattern's size S small, the following penalty function is introduced:

$$P = w_e \cdot \frac{E_{max}}{E_0} + w_s \cdot \frac{S}{S_0}, \quad (2)$$

where $E_0 = 5$ kJ/cm^3 (estimated damage threshold of the material) and $S_0 = 0.6$ (typical realistic pattern size) are scaling factors to normalize the two quantities, and w_e and w_s are weights. The penalty function was minimized as a function of the parameters A_1, A_2, Δf and Δt for different values of w_e/w_s, keeping their sum $w_e + w_s = 1$ constant.

Figure 2 shows the optimized pattern for $w_e/w_s = 0.125$, which gives a good compromise between the energy density and the size of the pattern. Results at different w_e/w_s values

* facsko.benedek@wigner.hu

ISBN: 978-3-95450-214-1 ISSN: 2673-5490 doi:10.18429/JACoW-IPAC2021-THPAB031

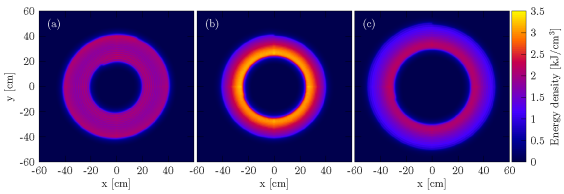

Figure 2: Energy density map of three patterns: (a) the optimized pattern using beating frequencies, (b) exponentially damping spiral with the same maximum excursion, and (c) with the same maximum energy density.

give preference to either a smaller dump absorber, or smaller energy deposition density. While using the exact same hardware (i.e. independent kicker circuits), the application of beating frequencies can reduce the required dump size by 18%, and the total needed strength of kickers by 13%.

BEAMLINE OPTIMIZATION

The goal of this work is to find the most effective, most reliable, cheap and simple layout. For individual dilution kicker magnets this means reducing the gap between their pole tips (A_v, "vertical aperture") to the minimum in order to keep the required current low for the same magnetic field, and keeping the distance between the conductors (A_h, "horizontal aperture") small in order to keep the voltage low. Efficient design, manufacturing, maintenance and spare unit management call for disfavouring the diversity of hardware. The goal of this work was therefore to find a beamline configuration which has at most 2 different types of kicker magnets (preferably only 1 type), even at the cost of an increased number of magnets. In a similar spirit, quadrupole magnets should be chosen from the existing designs used in the main ring, defined by their aperture, length and operational gradient, which should not be exceeded. As a baseline, the main quadrupoles [2] were chosen.

Baseline Layout

This layout was already studied before, and was found to be a feasible solution [3], but had not been optimized so far. This layout has the following configuration: (1) Quadrupole magnet: (Q_1 in Fig. 3) eliminates the uncertainties of the extraction kickers. (2) First set of kickers, non-extraction plane (NEP): (K_1 in Fig. 3). (3) Second set of quadrupole magnets: (Q_2, Q_3 and Q_4 in Fig. 3) to mitigate the problem of increasing beam size, affecting downstream kickers' aperture, in the non-extraction plane. (4) Second set of kickers, extraction plane (EP): (K_2 in Fig. 3), with the same parameters as K_1.

The quadrupole Q_1 is placed as upstream as possible, and its gradient is determined such that it images the extraction kicker to the location of the quadrupole triplet. Kickers K_1 (NEP) are placed after Q_1. The pole-tip distance (A_v) of these kickers is determined from the maximum of the beam envelope in the extraction plane along the set (taking into account the beam size and the uncertainties of to the extraction kicker waveform). Its other aperture (A_h), is determined so that the apertures of the two sets can be kept the same. Quadrupoles Q_2, Q_3 and Q_4 are placed after K_1. The first one's gradient is a free parameter, the other two have a gradient that produce the required pattern size at the dump target in the extraction plane. These quadrupoles are followed by the second kicker set, which is deflecting the beam in the extraction plane. To achieve the final pattern the needed angular change by these kickers is known. The parameters of the individual kicker magnets are required to be equal to the corresponding parameters of the first kickers (K_1). Their length l_2 is determined from the required deflection and their magnetic field (equal to the first set). The length of the drift spaces (D_1, D_2, D_3) are free parameters.

The optimized solution was chosen by minimizing the following penalty function, using a simplex algorithm:

$$\begin{aligned}\chi^2 = w_1 \cdot \sum_{i=1}^{4} \left(\frac{p_i}{p_0} - 1\right)^{10} \cdot (p_i > p_0) \\ + w_2 \cdot \frac{(l_1 + l_2)}{l_0} + w_3 \cdot \left(\frac{B_2}{B_1} - 1\right)^{10} \cdot (B_2 > B_1) \\ + w_4 \cdot \frac{d}{d_0} + w_5 \cdot \left(\frac{V}{V_0} - 1\right)^{10} \cdot (V > V_0)\end{aligned} \quad (3)$$

where w_i are weights. The first term penalizes quadrupole magnets which are stronger than the ring quadrupoles: p_0 is the pole-tip field of the main ring quadrupole, p_i is the pole-tip field for the quadrupoles. The second term penalizes long kicker sets, where $l_0 = 10$ m is the characteristic length of the two sets. The third term penalizes the case if the second set of kickers has a higher magnetic field than the first set: B_1 and B_2 are the magnetic fields of the first and second set. d is the maximum displacement of the beam at the target due to 10% over- or undershoot of the extraction kickers, and $d_0 = 1$ cm is the characteristic length of this displacement. V_0 is a target design voltage of the dilution kicker drive system, and V is the kicker voltage calculated from the kicker parameters. V_0 and the tunnel length l_t were external and not optimization parameters. The optimization algorithm minimizing the penalty function was executed for different values of V_0 and l_t, and the results will be displayed as a function of these parameters.

Alternating Kickers

In the baseline layout the horizontal and vertical kickers are arranged in two different groups at two different locations. This created asymmetrical aperture requirements for the two groups. This asymmetry can be eliminated, and the aperture requirements homogenized between the horizontal and vertical kickers, if they are arranged in an alternating pattern. In this way the three quadrupoles between the two groups of kickers can also be eliminated, the cryogenic installation can be saved.

The drawback of this concept is that the beam is not focused after the first quadrupole, and its envelope is constantly growing throughout the kickers. As a consequence, if a single type of kicker magnet is to be used, a longer set

ISBN: 978-3-95450-214-1 ISSN: 2673-5490 doi:10.18429/JACoW-IPAC2021-THPAB031

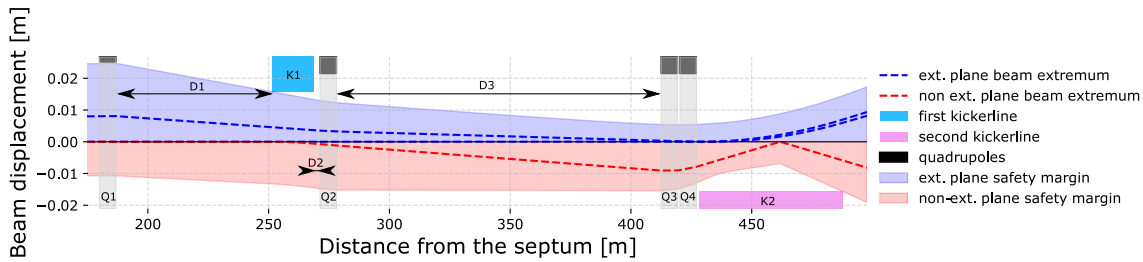

Figure 3: Optimized baseline layout for kicker voltage V_0=20 kV and tunnel length l_t=2 km. The dashed lines show the beam trajectories associated with the maximum excursion of the dilution pattern, and the shaded zones indicate the beam stay clear distance around these trajectories.

of kickers means a larger aperture, which in turn leads to a weaker magnetic field with the same inductive magnet voltage, and would thereby require more magnets. This vicious circle can lead to no solution for the problem, or too high requirements on the magnet current. Therefore in the following analysis up to two sets of kickers with different apertures were allowed.

For identically sized kickers, the assumed number of kicker magnets was increased in a loop, and their voltage was assumed to be V_0, a target design voltage of the system. At each step of the loop, their aperture was decreased from a large starting value until the beam stay clear distance around the deflected beam has hit the edge of the aperture at exit. For the calculation of the deflected beam's trajectory the magnetic field of the magnet was used, which changes inversely proportionally to the aperture. The loop was terminated when the required deflection to realize the optimal dilution pattern at the target was reached. For two sets of kickers the algorithm used nested loops. For a number n_1 of kickers in the first set (with aperture $A_v = A_h = A_1$) the number of kickers n_2 in the second set, with apertures $A_v = A_h = A_2$ was determined as described above. The algorithm was executed for several values of n_1, and the solution with the smallest value of $n_1 + n_2$ was chosen.

The algorithm defining the layout of the alternating kicker configuration is therefore a direct method. As for the baseline configuration, it was executed for different values of the target design voltage V_0 and tunnel length l_t, and the results will be displayed as a function of these parameters.

Results and Discussion

The total number of required kicker magnets is shown in Fig. 4 as a function of tunnel length l_t and target system voltage V_0. Since the voltage-term of the penalty function, Eq. (3) only penalizes cases where the magnet voltage exceeds the target voltage V_0 but does not prohibit it, the actual voltages in the baseline configuration can be larger than than V_0. Solutions where the voltage exceeded the target value by more than 0.2 kV were dropped and are not displayed in Fig. 4a. For the alternating kickers configuration, the actual magnet voltage equals V_0 by construction (Fig. 4).

As expected, the number of required kickers decreases with increasing tunnel length and system voltage. Although

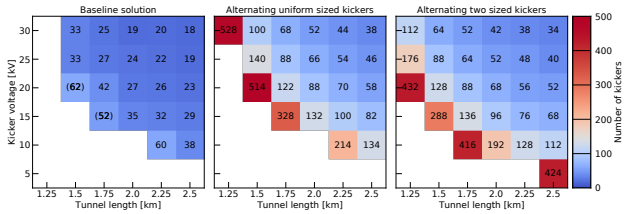

Figure 4: Required number of kicker magnets for different layouts.

the required number of kickers is significantly and systematically larger for the alternating configurations than for the baseline configuration, the alternating configurations offer the absence of cryogenic installations in the beamline. The construction and operational costs of, and the increased complexity due to this extra hardware must be taken into account when choosing between the two configurations. The difference in the number of kickers between the two alternating configurations is much less significant, and one must consider whether a somewhat smaller number of kickers, or a unique kicker magnet type is of more benefit.

Concerning the studied voltage range: the lower end (5 kV) would result in cheap and simple hardware in large quantities. The other end, 30 kV is close to the LHC dilution kickers' voltage, and leads to a lower number of magnets, at the cost of more expensive power supplies and high-voltage protection, a larger probability of a failing module and a larger relative effect of it. The results of the current work are therefore presented in a way which leaves the decision in this trade-off between price and reliability to a later point, when more is known about the hardware.

ACKNOWLEDGEMENTS

The authors are grateful to Mike Barnes and Wolfgang Bartman for their input and useful discussions. This research has received funding from the Hungarian National Research, Development and Innovation Office under grant # K124945.

REFERENCES

[1] B. Facskó, D. Barna, A. Lechner, and E. Renner, "Realization of the optimal beam dilution pattern of the FCC-hh ring using beating frequencies", *Nucl. Instrum. Methods Phys. Res., Sect.*

ISBN: 978-3-95450-214-1 ISSN: 2673-5490 doi:10.18429/JACoW-IPAC2021-THPAB031

A, vol. 992, no. 11, p. 165048, 2021. doi:10.1016/j.nima.2021.165048

[2] M. Benedikt *et al.*, "FCC-hh: The hadron collider - Future circular collider conceptual design report volume 3", *Eur. Phys. J. Spec. Top.*, vol. 228, pp. 755–1107, 2019. doi:10.1140/epjst/e2019-900087-0

[3] W. Bartman, private communication, Oct. 2020.